Helical ribbons tuned by alkoxy chains in achiral twin-tapered dihydrazide derivatives†

Songnan Qu, Haitao Wang, Zhixin Yu, Binglian Bai and Min Li*

Received (in Montpellier, France) 3rd April 2008, Accepted 10th June 2008
First published as an Advance Article on the web 5th August 2008
DOI: 10.1039/b805593a

Achiral twin-tapered dihydrazide derivatives (FH-T*n*, *n* = 3, 4, 5, 6, 7, 8, 10) are effective gelators in ethanol. The gelling ability in ethanol, the morphologies, packing structures and intermolecular H-bonding strength were significantly influenced by the length of the alkyl chains. FH-T6 and FH-T7 showed strong gelation ability in ethanol with critical gelation concentrations of 2.1×10^{-3} mol L^{-1} and 2.1×10^{-3} mol L^{-1}, respectively. Both left- and right-handed helical ribbons with non-uniform helical pitch were observed in FH-T*n* (*n* = 5, 6, 7) gels.

Introduction

Chirality plays an important role in life and material sciences. The chirality of a system involves intrinsically chiral molecules and chiral assemblies.[1] A chiral molecule has an asymmetric carbon atom or conformational asymmetry. Chiral assemblies are often achieved by non-covalent interactions between chiral molecules or between chiral building blocks.[2] Besides chiral molecules, achiral molecules can also contribute to the chirality of the supramolecular assemblies. The phenomenon that chiral supramolecular assemblies from achiral molecules is known as spontaneous symmetry breaking. To date it has been observed in various assemblies such as liquid crystals,[3] Langmuir–Blodgett films,[4] crystals[5] and organogels.[6] In these cases the symmetry breaking is explained by packing restrictions between different parts of the molecules or by the interplay of surface and volume effects.

Organogels are the materials in which three-dimensional networks are formed through self-assembling of low-molecular-weight compounds (organogelators) through non-colvalent interactions, and the network can absorb a large amount of solvent. Recently, the supramolecular architectures found in organogels attracted broad attention for the preparation of helical fibers or ribbons, in which the chiral groups (such as chiral alkyl chains,[7] amino acids,[8] glucose,[9] and cholesterol[10]) in the molecules can influence the formation of helices. However, few reports have described the formation of an artificial helix from achiral organogelators.[6]

Recently, we reported the synthesis and self-assembly of twin-tapered dihydrazide derivatives, oxalyl acid *N*′,*N*′-di(3,4,5-trialkoxybenzoyl)hydrazide (FH-T*n*),[11] as shown in Scheme 1, which self-assembled into supramolecular chains either in chloroform at concentrations higher than 255 μM or in bulk through intermolecular quadruple H-bonding, and these results suggested that bi-dihydrazide units could be used as self-complementary quadruple hydrogen-bonding units to assemble new supramolecules. In this work, we report gelation behaviors of FH-T*n* (*n* = 3, 4, 5, 6, 7, 8, 10). All the compounds formed stable gels in ethanol; the gelling ability in ethanol, the morphologies, packing structures and intermolecular H-bonding strength were significantly influenced by the length of the alkyl chains. Notably, both left- and right-handed helical ribbons with non-uniform helical pitch were generated by tuning the length of the alkoxy chains instead of any chiral groups.

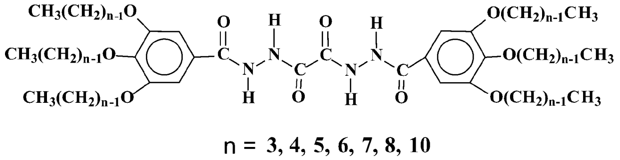

Scheme 1 Molecular structures of FH-T*n* (*n* = 3, 4, 5, 6, 7, 8, 10).

Results and discussion

The gels of FH-T*n* were prepared by mixing a weighed sample with solvent in a sealed test tube and heating the mixture until the solid dissolved and then this was cooled to 4 °C. The gelling properties of FH-T*n* in different solvents are summarized in Table 1. All the FH-T*n* formed stable gel in ethanol, while FH-T8 also gelled chloroform and benzene. It can be found that the length of the terminal alkoxy chains greatly affected the gelation ability in ethanol. FH-T6 and FH-T7 showed strong gelation ability in ethanol with critical gelation concentrations (CGC) of 2.1×10^{-3} and 2.3×10^{-3} mol L^{-1}, respectively, while both FH-T8 and FH-T10 exhibited relatively high CGCs, which are 1.0×10^{-2} and 1.1×10^{-2} mol L^{-1}, suggesting poor gelation ability. Fig. 1 shows the melting temperature (T_m) of FH-T6 gel in ethanol as a function of concentration. T_m values were determined by the "falling drop" method.[12] The T_m increases from 17 °C for the gel at 2.1×10^{-3} mol L^{-1} to 44 °C at 1.3×10^{-2} mol L^{-1}.

In order to investigate the aggregation morphology of the organogels, the xerogels FH-T*n* (*n* = 3, 4, 5, 6, 7, 8, 10) in

---

Key Laboratory of Automobile Materials (Jilin University), Ministry of Education, Institute of Materials Science and Engineering, Jilin University, Changchun 130012, P. R. China.
E-mail: minli@mail.jlu.edu.cn; Tel: +86 431 85168254

† Electronic supplementary information (ESI) available: SEM images and XRD patterns of FH-T8 xerogels from chloroform and benzene. Optical textures observed for FH-T4 and FH-T8 xerogels from ethanol. XRD pattern of FH-T5 film casted from chloroform. See DOI: 10.1039/b805593a

Table 1 Gelation properties of FH-T*n* (n = 3, 4, 5, 6, 7, 8, 10)[a]

	Ethanol	Acetone	Chloroform	Benzene
FH-T3	9.4×10^{-3}	S	S	S
FH-T4	5.2×10^{-3}	P	S	S
FH-T5	4.8×10^{-3}	P	S	S
FH-T6	2.1×10^{-3}	P	S	S
FH-T7	2.3×10^{-3}	P	S	S
FH-T8	1.0×10^{-2}	P	2.5×10^{-2}	1.4×10^{-2}
FH-T10	1.1×10^{-2}	P	P	S

[a] Values denote the minimum gel concentration (mol L^{-1}) necessary for organogelation. S: soluble, P: precipitation.

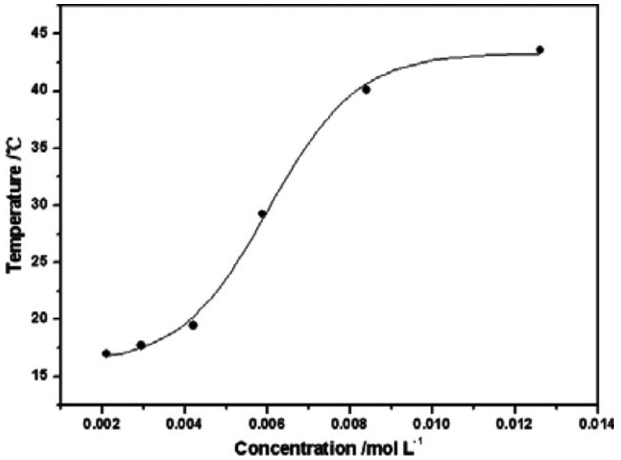

Fig. 1 Concentration-dependent melting temperature of FH-T6 gels in ethanol.

ethanol were prepared and subjected to scanning electron microscopy (SEM). As shown in Fig. 2a and 2b, FH-T3 xerogel from ethanol consists of bundles of flexible ribbons with the width of 0.3–2 μm, while FH-T4 xerogel consists of bundles of straight ribbons with the width of 1–2 μm. The formation of elongated ribbon-like aggregates indicates that self-assembly of FH-T*n* is driven by strong directional intermolecular interactions. Interestingly, both right- and left-handed helical ribbons with widths of 1–4 μm, 0.2–1 μm and 0.3–1 μm, respectively were observed for FH-T5, FH-T6 and FH-T7 xerogels (Fig. 2c–e). In some cases, superhelical ribbons composed of several helical ribbons were observed. In these samples, the helical pitches were non-uniform and some straight ribbons were also observed, indicating that the helical structures were not from a chiral center. Furthermore, left- and right-handed helical ribbons were present in equal quantities, thus resulting in overall racemic mixtures, which were confirmed by the absence of any CD signal (Fig. S6, ESI†). The helical structures were observed using polarizing optical microscopy (POM), in which the single ribbons of FH-T7 gel exhibited periodical repetitions of strongly birefringent regions and dark regions (Fig. 2f). No helical structure was observed, while only flat ribbons were observed for FH-T8 and FH-T10 (Fig. 2g and 2h). In the thermal gravimetric analysis (TGA) on xerogel of FH-T7, almost no losses of thermograms weight were detected upon heating to its isotropic point (177 °C), indicating that there is no ethanol in the xerogel (Fig. 3).

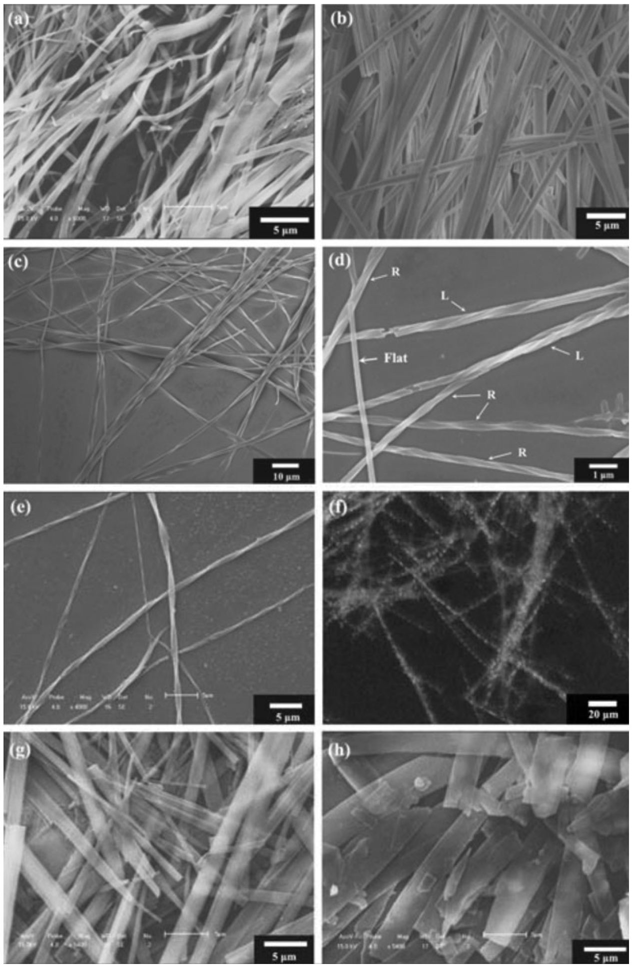

Fig. 2 SEM images of xerogels from (a) FH-T3 (1.0×10^{-2} mol L^{-1}), (b) FH-T4 (7.8×10^{-3} mol L^{-1}), (c) FH-T5 (6.7×10^{-3} mol L^{-1}), (d) FH-T6 (5.0×10^{-3} mol L^{-1}), (e) FH-T7 (4.6×10^{-3} mol L^{-1}), (g) FH-T8 (1.3×10^{-2} mol L^{-1}) and (h) FH-T10 (1.2×10^{-2} mol L^{-1}) in ethanol; (f) optical textures observed for FH-T7 gel in ethanol (4.6×10^{-3} mol L^{-1}).

The XRD patterns of the xerogels from FH-T*n* (n = 3, 4, 5, 6, 7, 8, 10) in ethanol were shown in Fig. 4. Many sharp diffraction peaks in both the low- and high-angle range were observed for FH-T*n* (n = 3, 4, 6, 7, 8, 10) xerogels indicating

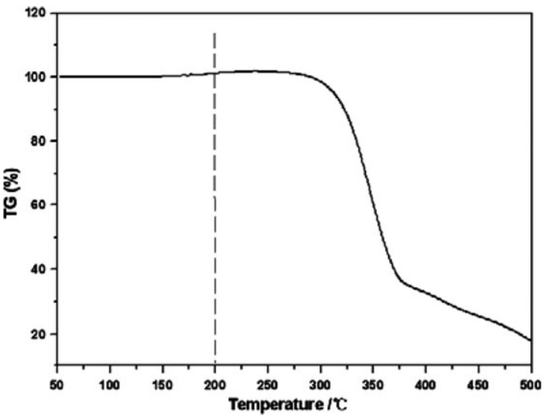

Fig. 3 TGA curve of FH-T7 xerogel from ethanol (4.6×10^{-3} mol L^{-1}).

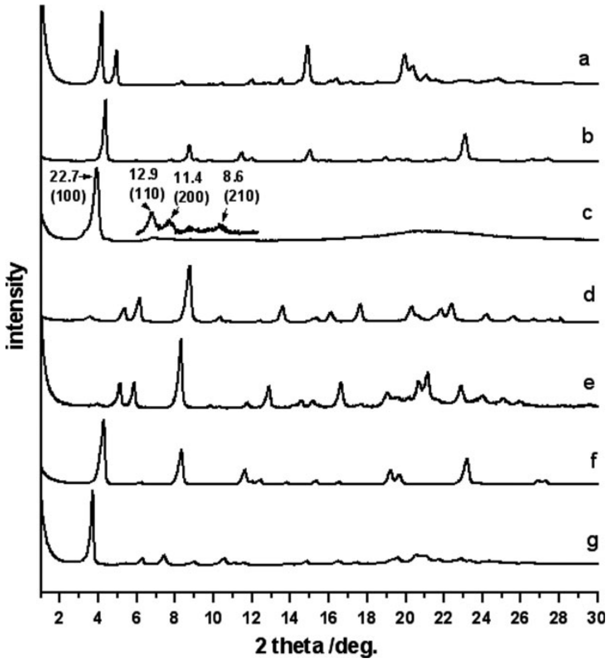

Fig. 4 XRD patterns of xerogels from (a) FH-T3 (1.0×10^{-2} mol L^{-1}), (b) FH-T4 (7.8×10^{-3} mol L^{-1}), (c) FH-T5 (6.7×10^{-3} mol L^{-1}), (d) FH-T6 (5.0×10^{-3} mol L^{-1}), (e) FH-T7 (4.6×10^{-3} mol L^{-1}), (g) FH-T8 (1.3×10^{-2} mol L^{-1}) and (h) FH-T10 (1.2×10^{-2} mol L^{-1}) in ethanol.

their crystalline feature, while xerogel FH-T5 exhibited one strong peak (22.7 Å) and three weak peaks (12.9, 11.4, 8.6 Å) in the high-angle range corresponding to a hexagonal columnar arrangement and a diffuse halo in the high-angle range indicating the packing of the alkoxy chains were disordered. In addition, a similar hexagonal columnar arrangement can also be observed by air-drying the chloroform solutions of FH-T5, indicating a similar supramolecular arrangement to that proposed in our previous work. Given the XRD patterns differences between the gels, it can be concluded that the length of the alkoxy chains have a significant effect on their packing modes during gelling in ethanol.

To investigate the interactions and alkyl chain conformations in the gels, FT-IR spectroscopy on organogels and xerogels of FH-T*n* (n = 3, 4, 5, 6, 7, 8, 10) in ethanol were performed. The FT-IR spectra of FH-T*n* organogels in ethanol were shown in Fig. S7, ESI†. Bands of N–H stretching vibrations and $\nu_s(CH_2)$ and $\nu_{as}(CH_2)$ in organogels of FH-T*n* overlapped with those of either ν(O–H) or $\nu_s(CH_2)$ and $\nu_{as}(CH_2)$ from ethanol. The band of amide I in the organogels of FH-T*n* (n =3, 4, 5, 6, 7) appeared at around 1692, 1660 cm^{-1}, while that at 1695, 1656, 1635, 1609 cm^{-1} for the FH-T10 gel, which shifted to shorter wavenumbers in their corresponding xerogels, suggesting an increase of hydrogen bonding during evaporation of ethanol in FH-T*n* (n = 3, 4, 5, 6, 7) organogels. The band of amide I either in the organogel or in xerogel of FH-T8 in ethanol were almost the same. Table 2 presented the assignments of infrared frequencies for FH-T*n* xerogels. The presence of N–H stretching vibrations in 3255–3185 cm^{-1} in FH-T*n* xerogels (the absence of free N–H, a relatively sharp peak with the frequency higher than 3400 cm^{-1}), intense absorption of amide I at 1631–1608 cm^{-1}, and relatively weak absorption at 1688–1673 cm^{-1} indicated that the N–H groups are associated with C=O groups *via* N–H···O=C hydrogen bonding (Fig. 5).[13] The N–H stretching vibrations and absorption of amide I in FH-T3 and FH-T5 xerogels appeared in longer wavenumbers than that of other FH-T*n* (n = 4, 6, 7, 8, 10) xerogels, indicating weaker hydrogen bonding. $\nu_s(CH_2)$ and $\nu_{as}(CH_2)$ in FH-T5 xerogel appeared at 2860 and 2933 indicating disordered alkyl chains.[14] $\nu_s(CH_2)$ and $\nu_{as}(CH_2)$ in FH-T*n* (6, 7, 8, 10) appeared in shorter wavenumbers (2854–2852 cm^{-1} and 2928–2921 cm^{-1}, respectively) compared to that of FH-T5, indicating increased population of the *trans* conformation of alkyl chains.

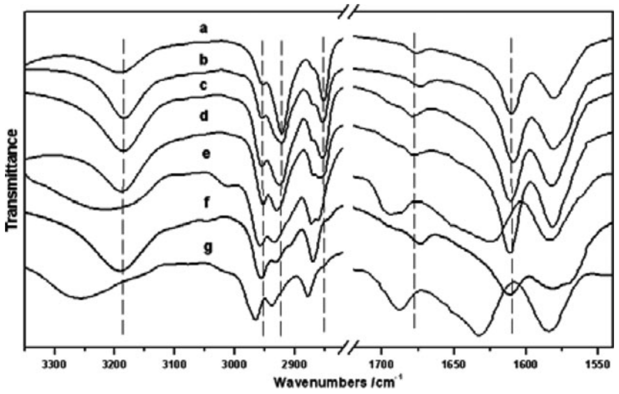

Fig. 5 FT-IR spectra of xerogels from (a) FH-T3 (1.0×10^{-2} mol L^{-1}), (b) FH-T4 (7.8×10^{-3} mol L^{-1}), (c) FH-T5 (6.7×10^{-3} mol L^{-1}), (d) FH-T6 (5.0×10^{-3} mol L^{-1}), (e) FH-T7 (4.6×10^{-3} mol L^{-1}), (g) FH-T8 (1.3×10^{-2} mol L^{-1}) and (h) FH-T10 (1.2×10^{-2} mol L^{-1}) in ethanol at room temperature.

Conclusion

The present work revealed that achiral twin-tapered dihydrazide derivatives (FH-T*n*, n = 3, 4, 5, 6, 7, 8, 10) are effective gelators in ethanol. The gelling ability in ethanol, the morphologies, packing structures and intermolecular H-bonding strength were significantly influenced by the length of the

Table 2 Assignments of infrared frequencies for FH-T*n* (n = 3, 4, 5, 6, 7, 8, 10) xerogels from ethanol

	IR frequencies/cm^{-1}						
Assignment	FH-T3	FH-T4	FH-T5	FH-T6	FH-T7	FH-T8	FH-T10
ν(N–H)	3255	3192	3209	3185	3185	3185	3187
$\nu_{as}(CH_3)$, $\nu_{as}(CH_2)$	2966, 2937	2956, 2932	2957, 2933	2953, 2928	2953, 2924	2953, 2922	2953, 2921
$\nu_s(CH_3)$, $\nu_s(CH_2)$	2877	2871	2872, 2860	2870, 2854	2870, 2853	2870, 2852	2870, 2852
Amide I, νC=O	1688, 1631	1673, 1610	1691, 1624	1677, 1610	1677, 1610	1673, 1608	1674, 1609

alkoxy chains. FH-T6 and FH-T7 showed strong gelation ability in ethanol with critical gelation concentrations of 2.1×10^{-3} and 2.3×10^{-3} mol L^{-1}, respectively. Both left- and right-handed helical ribbons with non-uniform helical pitch were observed in FH-T*n* (n = 5, 6, 7) gels. This new self-assembly of twin-tapered molecules containing bi-dihydrazide units will offer excellent opportunities for the organization of other functional groups.

Experimental

Experimental techniques

FT-IR spectra were recorded with a Perkin–Elmer spectrometer (Spectrum One B). The samples were pressed tablets with KBr. SEM observations were taken with a JSM-6700F apparatus or a SSX-550 apparatus. Optical textures were observed under polarized optical microscope (POM, Leica DMLP). X-Ray diffraction (XRD) studies were carried out with a Bruker Avance D8 X-ray diffractometer. Thermal gravimetry (TG) curves were measured on a TA SDTQ 600 instrument.

Acknowledgements

The authors are grateful to the National Science Foundation Committee of China (project No. 50373016), Program for New Century Excellent Talents in Universities of China Ministry of Education, Special Foundation for PhD Program in Universities of China Ministry of Education (Project No. 20050183057), and Project 985-Automotive Engineering of Jilin University for their financial support of this work.

References

1 H. G. Kuball and T. Höfer, *Chirality*, 2000, **12**, 278–286.
2 (*a*) A. E. Rowan and R. J. M. Nolte, *Angew. Chem., Int. Ed.*, 1998, **37**, 63–68; (*b*) J. H. K. K. Hirschberg, L. Brunsveld, A. Ramzi, J. A. J. M. Vekemans, R. P. Sijbesma and E. W. Meijer, *Nature*, 2000, **407**, 167–170.
3 (*a*) G. Pelzl, S. Diele and W. Weissflog, *Adv. Mater.*, 1999, **11**, 707; (*b*) A. Jákli, G. G. Nair, C. K. Lee, R. Sun and L. C. Chien, *Phys. Rev. E: Stat., Nonlinear, Soft Matter Phys.*, 2001, **63**, 061710; (*c*) M. Hird, J. W. Goodby, N. Gough and K. J. Toyne, *J. Mater. Chem.*, 2001, **11**, 2732; (*d*) K.-U. Jeong, B. S. Knapp, J. J. Ge, S. Jin, M. J. Graham, F. W. Harris and S. Z. D. Cheng, *Chem. Mater.*, 2006, **18**, 680–690; (*e*) Y. Takanishi, T. Izumi, J. Watanabe, K. Ishikawa, H. Takezoe and A. Iida, *J. Mater. Chem.*, 1999, **9**, 2771.
4 (*a*) J. Yuan and M. Liu, *J. Am. Chem. Soc.*, 2003, **125**, 5051–5056; (*b*) X. Huang, C. Li, S. Jiang, X. Wang, B. Zhang and M. Liu, *J. Am. Chem. Soc.*, 2004, **126**, 1322–1323; (*c*) X. Zhai, L. Zhang and M. Liu, *J. Phys. Chem. B*, 2004, **108**, 7180–7185; (*d*) L. Zhang, Q. Lu and M. Liu, *J. Phys. Chem. B*, 2003, **107**, 2565–2569; (*e*) P. Guo and M. Liu, *Langmuir*, 2005, **21**, 3410–3412.
5 (*a*) E.-Q. Gao, Y.-F. Yue, S.-Q. Bai, Z. He and C.-H. Yan, *J. Am. Chem. Soc.*, 2004, **126**, 1419–1429; (*b*) H. Koshima, S. Honke and J. Fujita, *J. Org. Chem.*, 1999, **64**, 3916–3921; (*c*) Y. Inai, T. Oshikawa, M. Yamashita, K. Tagawa and T. Hirabayashi, *Biopolymers*, 2003, **70**, 310–322.
6 (*a*) C. Bao, R. Lu, M. Jin, P. Xue, C. Tan, T. Xu, G. Liu and Y. Zhao, *Chem.–Eur. J.*, 2006, **12**, 3287–3294; (*b*) J. van Esch, S. D. Feyter, R. M. Kellogg, F. D. Schryver and B. L. Feringa, *Chem.–Eur. J.*, 1997, **3**, 1238–1243.
7 (*a*) L. Brunsveld, H. Zhang, M. Glasbeek, J. A. J. M. Vekemans and E. W. Meijer, *J. Am. Chem. Soc.*, 2000, **122**, 6175–6182; (*b*) J. J. Van Gorp, J. A. J. M. Vekemans and E. W. Meijer, *J. Am. Chem. Soc.*, 2002, **124**, 14759–14769; (*c*) H. Engelkamp, S. Middelbeek and R. J. M. Nolte, *Science*, 1999, **284**, 785–788; (*d*) S. J. George, A. Ajayaghosh, P. Jonkheijin, A. P. H. J. Schenning and E. W. Meijer, *Angew. Chem.*, 2004, **116**, 3504–3507; S. J. George, A. Ajayaghosh, P. Jonkheijin, A. P. H. J. Schenning and E. W. Meijer, *Angew. Chem., Int. Ed.*, 2004, **4300**, 3422–3425; (*e*) S. J. Lee, S. S. Lee, J. S. Kim, J. Y. Lee and J. H. J, *Chem. Mater.*, 2005, **1700**, 6517–6520.
8 (*a*) T. Sagawa, S. Fukugawa, T. Yamada and H. Ihara, *Langmuir*, 2002, **18**, 7223–7228; (*b*) L. A. Estroff and A. D. Hamilton, *Angew. Chem.*, 2000, **112**, 3589–3592; L. A. Estroff and A. D. Hamilton, *Angew. Chem., Int. Ed.*, 2000, **39**, 3447–3450; (*c*) G. Palui, F. X. Simon, M. Schmutz, P. J. Mesini and A. Banerjee, *Tetrahedron*, 2008, **64**, 175–185.
9 (*a*) I. Nakazawa, M. Masuda, Y. Okada, T. Hanada, K. Yase, M. Asai and T. Shimizu, *Langmuir*, 1999, **15**, 4757–4764; (*b*) G. John, M. Masuda, Y. Okada, K. Yase and T. Shimizu, *Adv. Mater.*, 2001, **13**, 715–718; (*c*) G. John, J. H. Jung, H. Minamikawa, K. Yoshida and T. Shimizu, *Chem.–Eur. J.*, 2002, **8**, 5494–5500; (*d*) S. Tamaru, S. Uchino, M. Takeuchi, M. Ikeda, T. Hatano and S. Shinkai, *Tetrahedron Lett.*, 2002, **43**, 3751–3755.
10 (*a*) P. C. Xue, R. Lu, D. M. Li, M. Jin, C. H. Tan, C. Y. Bao, Z. M. Wang and Y. Y. Zhao, *Langmuir*, 2004, **20**, 11234–11239; (*b*) E. Snip, K. Koumoto and S. Shinkai, *Tetrahedron*, 2002, **58**, 8863–8873; (*c*) J. H. Jung, S. Shinkai and T. Shimizu, *Chem. Mater.*, 2003, **15**, 2141–2145; (*d*) P. C. Xue, R. Lu, D. M. Li, M. Jin, C. Y. Bao, Y. Y. Zhao and Z. M. Wang, *Chem. Mater.*, 2004, **16**, 3702–3707; (*e*) S. Kawano, N. Fujita and S. Shinkai, *J. Am. Chem. Soc.*, 2004, **126**, 8592–8593.
11 (*a*) S. Qu, F. Li, H. Wang, B. Bai, C. Xu, L. Zhao, B. Long and M. Li, *Chem. Mater.*, 2007, **19**, 4839–4846; (*b*) S. Qu and M. Li, *Tetrahedron*, 2007, **63**, 12429–12436.
12 D. J. Abdallah and R. G. Weiss, *Langmuir*, 2000, **16**, 352.
13 (*a*) D. J. Skrovanek, S. E. Howe, P. C. Painter and M. M. Coleman, *Macromolecules*, 1985, **18**, 1676–1683; (*b*) P. I. Harris and D. Chapman, *Biopolymers*, 1995, **37**, 251–263.
14 (*a*) R. G. Snyder, H. L. Strauss and C. A. Elliger, *J. Phys. Chem.*, 1982, **86**, 5145–5150; (*b*) R. A. MacPhail, H. L. Strauss, R. G. Snyder and C. A. Elliger, *J. Phys. Chem.*, 1984, **88**, 334–341; (*c*) N. V. Venkataraman and S. Vasudevan, *J. Phys. Chem. B*, 2001, **105**, 1805–1812.